THERMOELASTIC STRESSES IN TUBES PRODUCED FROM A MELT BY STEPANOV'S METHOD

A. V. Zhdanov, V. A. Borodin, and L. P. Nikolaeva

UDC 539.32

Temperature fields and their corresponding thermoelastic stresses in tubes in the process of their growth from a melt by Stepanov's method are calculated. Results of the calculations are presented in the form of surfaces constructed above a longitudinal section of a tube. The behavior of the maximal stresses as a function of the tube length, the middle radius, and the wall thickness is investigated. The influence of the screen on the stress distribution is also taken into account.

Introduction. Tubes grown from a melt by Stepanov's method have widespread technical application. In particular, sapphire tubes are used as bulbs of gas-discharge tubes, in laser engineering, in fine chemical technology, and in high-vacuum equipment. Practice has shown that angles of disorientation of smallangle boundaries in sapphire tubes may not exceed several degrees, since as the disorientation angles between blocks increase, the strength and dielectric properties of these crystals drastically deteriorate. One of the basic mechanisms for formation of the block structure of melt-grown crystals, including profiled sapphire ones, is polygonization of dislocations, which begins when the dislocation density exceeds some critical value [1-3]. Dislocations, in turn, form with deformations caused by thermal stresses. Calculations of the temperature fields in tubes and their corresponding thermoelastic stresses make it possible to obtain initial data for improving and optimizing the process of growth. In the present work thermoelastic stresses in sapphire tubes are calculated as a function of the heat transfer conditions and the parameters of the tube. Heat transfer with the external medium in the process of growth depends, of course, on whether the grown tube is in the zone surrounded by the screen or partially goes out of the zone at some length. Both these cases are considered. The developed approach is promising for calculating thermoelastic stresses from the experimental dependences of the ambient temperature along the lateral surfaces of the tube.

The case of a semiinfinite tube using a one-dimensional approximation of the temperature field is given in [4]. Our work also takes into account the influence of the second end of the tube on the distribution of stresses, which can be very large. A number of interesting results on calculation and experimental investigations of thermal fields and their related thermoelastic stresses in growing crystals of various shapes is presented in [6].

1. **Mathematical Model.** We consider the process of crystallization from a melt, which consists in producing a tube having the inner radius R_1 and the outer one R_2. From the experimental data the pull rate V_0 and the temperature regime of a thermal node are assumed known. Owing to the smallness of the pull rate we will consider the problem of determination of the temperature field $T(r, z)$ in the crystal in a quasistationary approximation. We introduce a cylindrical system of coordinates r, z, whose z axis is directed along the symmetry axis of the tube and whose origin is at the center of the lower end of the tube. Then the temperature $T(r, z)$ satisfies the following heat conduction equation:

$$k_s\nabla \nabla T - V_0\rho_s c_{\rho s} e_z \nabla T = 0. \tag{1}$$

On the inner $(r = R_1)$ and outer $(r = R_2)$ surfaces of the tube the heat transfer with the external medium having the temperatures Θ_1 and Θ_2 is prescribed:

$$-k_s\frac{\partial T}{\partial r} = h_s(T - \Theta_2)|_{r=R_2}, \quad k_s\frac{\partial T}{\partial r} = h_s(T - \Theta_1)|_{r=R_1}, \tag{2}$$

Institute of Physics of Solids of the Russian Academy of Sciences, Chernogolovka. Translated from Inzhenerno-Fizicheskii Zhurnal, Vol. 64, No. 4, pp. 469-476, April, 1993. Original article submitted January 23,

1062-0125/93/6404-0379$12.50

where

$$\Theta_1 = \begin{cases} T_1^0 + \frac{z}{l^*}(T_2^0 - T_1^0), & 0 \leqslant z \leqslant l^*, \\ \frac{T_5^0 - T_2^0}{l - l^*} z + \frac{T_2^0 l - T_5^0 l^*}{l - l^*}, & l^* \leqslant z \leqslant l; \end{cases}$$

$$\Theta_2 = \begin{cases} T_3^0 + \frac{z}{l^*}(T_4^0 - T_3^0), & 0 \leqslant z \leqslant l^*, \\ \frac{T_6^0 - T_4^0}{l - l^*} z + \frac{T_4^0 l - T_6^0 l^*}{l - l^*}, & l^* \leqslant z \leqslant l. \end{cases}$$

Here the screen height is denoted by l^* and the temperatures of the external medium outside and inside the tube at z = 0 are denoted by T_1^0 and T_3^0; similarly, T_5^0, T_6^0 and T_2^0, T_4^0 are the temperatures of the external medium at $z = l^*$ and $z = l$ respectively. These temperatures can be directly measured in the process of crystal growth. Thus, the ambient temperature is prescribed by a piecewise linear function. Besides, on the crystallization front z = 0 and on the upper end of the tube $z = l$ the temperatures are prescribed:

$$T(r, 0) = T_m, \quad T(r, l) = T_0, \quad R_1 \leqslant r \leqslant R_2. \tag{3}$$

We represent the solution of problem (1)-(3) as the sum

$$T(r, z) = T^*(r, z) + T_1(r, z), \tag{4}$$

where the function $T^*(r, z)$ satisfies just the boundary condition

$$-k_s \frac{\partial T^*}{\partial r} = h_s(T^* - \Theta_1)|_{r=R_1}, \quad k_s \frac{\partial T^*}{\partial r} = h_s(T^* - \Theta_2)|_{r=R_2}.$$

We will write such a function, satisfying, among other things, the equation $\Delta T^* = 0$, in the following manner:

$$T^*(r, z) = A(z) \ln r + C(z),$$

where the coefficients A(z) and C(z) have the form

$$A(z) = \lambda \frac{\Theta_2 - \Theta_1}{w_1 + w_2}, \quad C(z) = \frac{\Theta_1 w_2 + \Theta_2 w_1}{w_1 + w_2},$$

$$w_1 = \frac{1}{R_1} - \lambda \ln R_1, \quad w_2 = \frac{1}{R_2} + \lambda \ln R_2, \quad \lambda = \frac{h_s}{k_s}.$$

Then for the temperature $T_1(r, z)$ we will have a nonhomogeneous heat conduction equation, but, with homogeneous boundary conditions on the inner and outer tube surfaces. To determine $T_1(r, z)$, we apply the method of separation of variables, according to which the solution $T_1(r, z)$ is represented by a sum:

$$T_1(r, z) = \sum_{k=1}^{\infty} Z_k(z) X_k(r).$$

Here the functions $X_k(r)$ are determined by the formulas

$$X_k = \frac{D_k(r)}{\|D_k\|}, \quad D_k = D\left(\frac{\mu_k}{R_2} r\right) = J_0\left(\frac{\mu_k}{R_2} r\right) + \gamma(\mu_k) N_0\left(\frac{\mu_k}{R_2} r\right)$$

(J_0, N_0 are zero-order Bessel functions of the 1st and 2nd kinds respectively). The proper values μ_k are solutions of the algebraic equation

$$\begin{vmatrix} \mu J_1(\mu) - kJ_0(\mu), & \mu N_1(\mu) - kN_0(\mu) \\ \mu J_1\left(\mu \frac{R_1}{R_2}\right) + kJ_0\left(\mu \frac{R_1}{R_2}\right), & \mu N_1\left(\mu \frac{R_1}{R_2}\right) + kN_0\left(\mu \frac{R_1}{R_2}\right) \end{vmatrix} = 0,$$

and the numbers $\gamma(\mu_k)$ are equal to

$$\gamma(\mu_k) = -\frac{\mu_k J_1(\mu_k) - kJ_0(\mu_k)}{\mu_k N_1(\mu_k) - kN_0(\mu_k)}.$$

The square of the norm of the function D_k is equal to

$$\|D_k\|^2 = \frac{(k^2+\mu_k^2)}{2\lambda_k}\left[D^2(\mu_k) - \left(\frac{R_1}{R_2}\right)^2 D^2\left(\mu_k \frac{R_1}{R_2}\right)\right], \quad k = \frac{\lambda}{R_2}.$$

The function Z_k satisfies the differential equation

$$Z_k'' - \chi Z_k' - \lambda_k Z_k = C_k, \quad \lambda_k = \left(\frac{\mu_k}{R_2}\right)^2, \quad \chi = \frac{V_0 \rho_s c_{\rho s}}{k_s} \tag{5}$$

with the boundary conditions

$$Z_k(0) = (T_m - T^*(0),\ X_k)_\rho = a_k, \quad Z_k(l) = (T_0 - T^*(l),\ X_k)_\rho = b_k.$$

Here the scalar product in the space $L_2(0, l)$ with the weight $\rho = r$ is denoted by $(. , .)_\rho$. The right side C_k in Eq. (5) has the form

$$C_k = -C_k^{(3)}\delta(z - l^*) + \begin{cases} C_k^{(1)}, & z \leqslant l^*, \\ C_k^{(2)}, & z > l^*, \end{cases}$$

where $\delta(z)$ is the Dirac delta-function,

$$\begin{gathered} C_k^{(i)} = \frac{\chi}{\|D_k\|\lambda_k}\Big[\{\alpha_i(k \ln R_2 + 1) + k\beta_i\} D(\mu_k) + \\ + \left\{\alpha_i\left(k\frac{R_1}{R_2}\ln R_1 - 1\right) + \beta_i k\frac{R_1}{R_2}\right\}\Big] D\left(\mu_k\frac{R_1}{R_2}\right), \quad i = 1,\ 2; \\ \alpha_1 = \lambda\frac{T_4^0 + T_1^0 - T_2^0 - T_3^0}{l^*(w_1 + w_2)}, \quad \alpha_2 = \lambda\frac{T_6^0 + T_2^0 - T_4^0 - T_5^0}{(l - l^*)(w_1 - w_2)}, \\ \beta_1 = \frac{(T_2^0 - T_1^0)w_2 + (T_4^0 - T_3^0)w_1}{l^*(w_1 + w_2)}, \quad \beta_2 = \frac{(T_5^0 - T_2^0)w_2 + (T_6^0 - T_4^0)w_1}{(l - l^*)(w_1 + w_2)}. \end{gathered} \tag{6}$$

The coefficients $C_k^{(3)}$ are calculated by formula (6); one needs only to take $(\alpha_2 - \alpha_1)$ instead of α_i and $(\beta_2 - \beta_1)$ instead of β_i and to assume χ equal to 1. The boundary values a_k and b_k are calculated in an explicit form and are equal to

$$\begin{gathered} a_k = \frac{1}{|D_k|\lambda_k}\left\{\delta_1 k\left[D(\mu_k) + \frac{R_1}{R_2} D\left(\mu_k\frac{R_1}{R_2}\right)\right] + \right. \\ \left. + \gamma_1\left[kD(\mu_k)\ln R_2 + k\frac{R_1}{R_2} D\left(\mu_k\frac{R_1}{R_2}\right)\ln R_1 + D(\mu_k) - D\left(\mu_k\frac{R_1}{R_2}\right)\right]\right\}, \end{gathered}$$

where

$$\delta_1 = T_m - \frac{T_1^0 w_2 + T_3^0 w_1}{w_1 + w_2}, \quad \gamma_1 = -\lambda\frac{T_3^0 - T_1^0}{w_1 + w_2}.$$

The coefficients b_k are calculated by the same formulas as a_k; one should only take δ_2 and γ_2 instead of δ_1 and γ_1. The values of δ_2 and γ_2 are calculated by the formulas

$$\delta_2 = T_0 - \frac{T_5^0 w_2 + T_6^0 w_1}{w_1 + w_2}, \quad \gamma_2 = -\lambda\frac{T_6^0 - T_5^0}{w_1 + w_2}.$$

And, finally, the functions $Z_k(z)$, by means of the notation introduced above, are written thus:

$$Z_k(z) = Z_k^{(0)} - Z_k^{(1)} + C_k^{(3)} G_k(z,\ l^*), \tag{7}$$

$$Z_k^{(0)} = a_k \frac{\exp\left(\frac{\chi z}{2}\right) \operatorname{sh} \frac{\eta_k (l-z)}{2}}{\operatorname{sh} \frac{\eta_k l}{2}} +$$

$$+ b_k \frac{\exp\left(\frac{\chi (z-l)}{2}\right) \operatorname{sh} \frac{\eta_k z}{2}}{\operatorname{sh} \frac{\eta_k l}{2}}, \quad \eta_k = \sqrt{\chi^2 + 4\lambda},$$

$$G_k(z,\ l^*) = \frac{2 \exp \frac{\chi (z - l^*)}{2}}{\eta_k \operatorname{sh} \frac{\eta_k l}{2}} \begin{cases} \operatorname{sh} \frac{\eta_k z}{2} \operatorname{sh} \frac{\eta_k (l - l^*)}{2}, & z \leqslant l^*, \\ \operatorname{sh} \frac{\eta_k (l-z)}{2} \operatorname{sh} \frac{\eta_k l^*}{2}, & z > l^*, \end{cases}$$

and the functions $Z_k^{(1)}$ are equal to

$$Z_k^{(1)} = \frac{\exp \frac{\chi z}{2}}{\lambda_k \operatorname{sh} \frac{\eta_k l}{2}} \left[\operatorname{sh} \frac{\eta_k (l-z)}{2} \left\{ \exp \frac{-\chi z}{2} \left[\frac{\chi}{\eta_k} \operatorname{sh} \frac{\eta_k z}{2} + \operatorname{ch} \frac{\eta_k z}{2} \right] - \right.\right.$$

$$\left. - 1 \right\} C_k^{(1)} + \operatorname{sh} \frac{\eta_k z}{2} \left\{ \exp \frac{-\chi l^*}{2} \left[\frac{\chi}{\eta_k} \operatorname{sh} \frac{\eta_k (l - l^*)}{2} - \operatorname{ch} \frac{\eta_k (l - l^*)}{2} \right] - \right.$$

$$\left. - \exp \frac{-\chi z}{2} \left[\frac{\chi}{\eta_k} \operatorname{sh} \frac{\eta_k (l-z)}{2} - \operatorname{ch} \frac{\eta_k (l-z)}{2} \right] \right\} C_k^{(1)} -$$

$$- \operatorname{sh} \frac{\eta_k z}{2} \left\{ \exp \frac{-\chi l^*}{2} \left[\frac{\chi}{\eta_k} \operatorname{sh} \frac{\eta_k (l - l^*)}{2} - \operatorname{ch} \frac{\eta_k (l - l^*)}{2} \right] + \right.$$

$$\left.\left. + \exp \frac{-\chi l}{2} \right\} C_k^{(2)} \right], \quad z \leqslant l^*;$$

$$Z_k^{(1)} = \frac{\exp \frac{\chi z}{2}}{\lambda_k \operatorname{sh} \frac{\eta_k l}{2}} \left[\operatorname{sh} \frac{\eta_k (l-z)}{2} \left\{ \exp \frac{-\chi l^*}{2} \left[\frac{\chi}{\eta_k} \operatorname{sh} \frac{\eta_k l^*}{2} + \right.\right.\right.$$

$$\left.\left. + \operatorname{ch} \frac{\eta_k l^*}{2} \right] - 1 \right\} C_k^{(1)} + \operatorname{sh} \frac{\eta_k (l-z)}{2} \left\{ \exp \frac{-\chi z}{2} \left[\frac{\chi}{\eta_k} \operatorname{sh} \frac{\eta_k z}{2} + \right.\right.$$

$$\left.\left. + \operatorname{ch} \frac{\eta_k z}{2} \right] + \exp \frac{-\chi l^*}{2} \left[\frac{\chi}{\eta_k} \operatorname{sh} \frac{\eta_k l^*}{2} + \operatorname{ch} \frac{\eta_k l^*}{2} \right] \right\} C_k^{(2)} -$$

$$- \operatorname{sh} \frac{\eta_k z}{2} \left\{ \exp \frac{-\chi z}{2} \left[\frac{\chi}{\eta_k} \operatorname{sh} \frac{\eta_k (l-z)}{2} - \operatorname{ch} \frac{\eta_k (l-z)}{2} \right] + \right.$$

$$\left.\left. + \exp \frac{-\chi l}{2} \right\} C_k^{(2)} \right], \quad z > l^*.$$

In order to calculate the thermoelastic stress-strain state, we represent the tube as a circular cylindrical shell of constant thickness. We denote the shell thickness by $h = R_1 - R_2$, the middle- surface radius by $R = \frac{R_1 + R_2}{2}$, the axial and radial travel of the middle surface by u and ω respectively, and the meridian and radial normal stresses by σ_m and σ_φ.

The temperature stresses σ_m and σ_φ are determined from the known formulas [5]

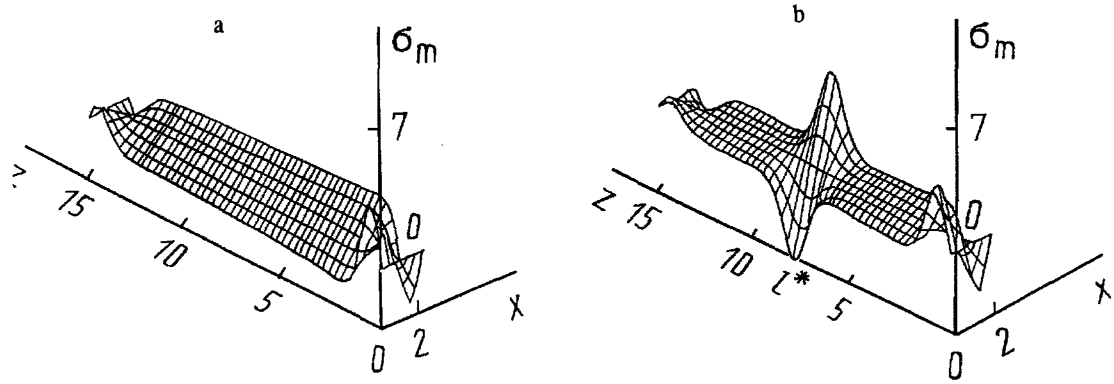

Fig. 1. Typical distribution of the normal meridian stress σ_m: a) without screen; b) with a screen. σ_m, kg/mm^2; z, cm; x, mm.

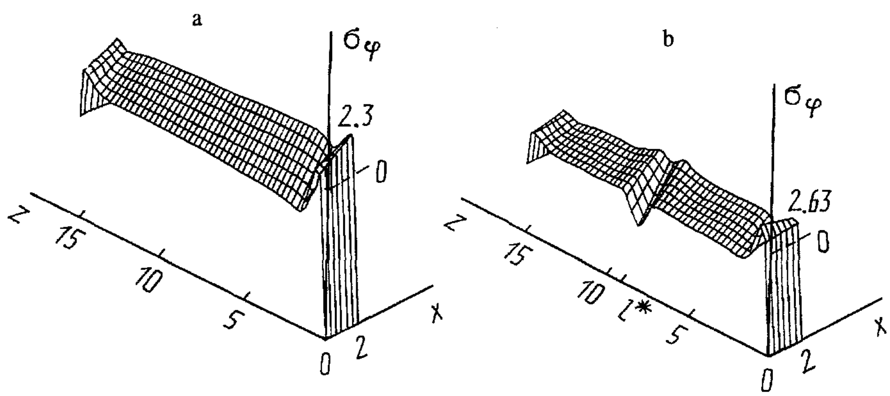

Fig. 2. Typical distribution of the normal hoop stress σ_φ: a) without screen; b) with a screen. σ_φ, kg/mm^2.

$$\sigma_m = \frac{E}{1-\nu^2}\left[\frac{du}{dz} - x\frac{d^2\omega}{dz^2} + \nu\frac{\omega}{R} - (1+\nu)\,\alpha_t T\right],$$

$$\sigma_\varphi = \frac{E}{1-\nu^2}\left[\nu\frac{du}{dz} - \nu x\frac{d^2\omega}{dz^2} + \frac{\omega}{R} - (1+\nu)\,\alpha_t T\right],$$

$$u = \int\left[(1+\nu)\overline{T} - \nu\frac{\omega}{R}\right]dz, \quad M = -D\left[\frac{d^2\omega}{dz^2} + (1+\nu)\,\alpha_t\overline{\overline{T}}\right].$$

The quantity x in formulas (8) is reckoned from the middle surface of the tube ($-0.5h \leq x \leq 0.5h$). The components of the vector of travel ω satisfy the equation

$$\frac{d^4\omega}{dz^4} + 4k^4\omega = \frac{Eh\alpha_t}{DR}\overline{T} - (1+\nu)\,\alpha_t\frac{d^2\overline{\overline{T}}}{dz^2} \overset{\text{def}}{=} f(z). \tag{9}$$

In Eq. (9) the expressions for $\overline{T}$ and $\overline{\overline{T}}$ are defined by the equalities

$$\overline{T} = \frac{1}{h}\int_{-h/2}^{h/2} T(R+x,\ z)\,dx, \quad \overline{\overline{T}} = \frac{12}{h^3}\int_{-h/2}^{h/2} T(R+x,\ z)\,x\,dx.$$

The boundary conditions for Eq. (9) are formulated for a shell with free edges, i.e.,

$$M = \frac{dM}{dz} = 0, \quad z = 0,\ l. \tag{10}$$

We write the general solution of Eq. (9) as

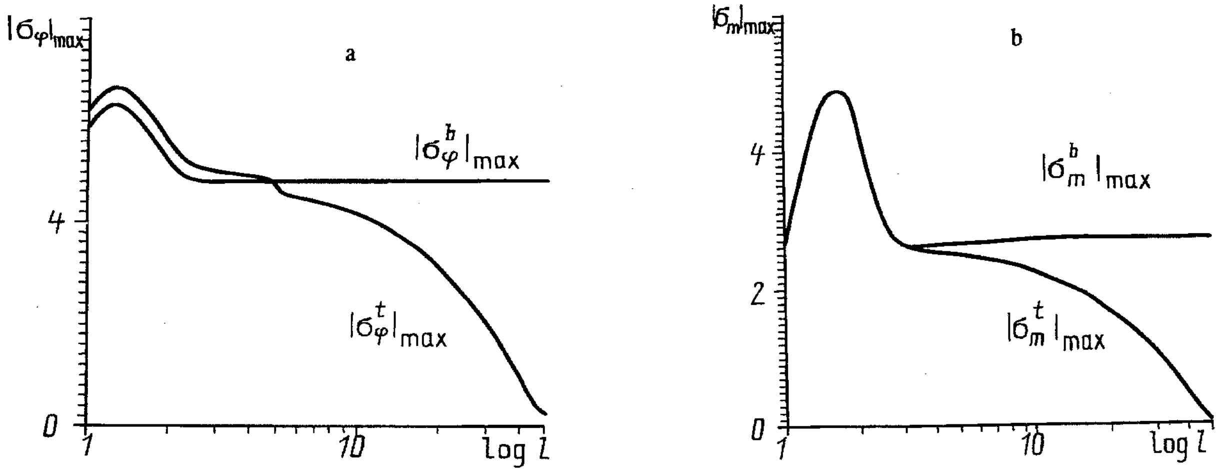

Fig. 3. Dependence of $|\sigma_\varphi|_{max}$ (a) and $|\sigma_m|_{max}$ (b) on the crystal length. $|\sigma_\varphi|_{max}$, $|\sigma_m|_{max}$, kg/mm^2; log l, cm.

$$\omega(z) = C_1 \operatorname{sh} kz \cos kz + C_2 \frac{1}{2}[\operatorname{ch} kz \sin kz + \operatorname{sh} kz \cos kz] +$$
$$+ C_3 \frac{1}{2} \operatorname{sh} kz \sin kz + C_4 \frac{1}{4}[\operatorname{ch} kz \sin kz - \operatorname{sh} kz \cos kz] +$$
$$+ \frac{1}{4k^3} \int_0^z [\operatorname{ch} k(z-\xi) \sin(z-\xi) - \operatorname{sh}(z-\xi) \cos(z-\xi)] f(\xi)\, d\xi.$$

The coefficients C_1, C_2, C_3, C_4 are found from boundary conditions (10). In formulas (8) and (9) by k, D we denoted

$$k^4 = \frac{3(1-\nu^2)}{h^2R^2}, \quad D = \frac{Eh^3}{12(1-\nu^2)}.$$

We give the characteristics of the materials and parameters of the process:

T_m^0=2050 °C; k_s=0.015 cal/(cm·sec·deg); ρ_s=4 g/cm^3; $\alpha_t=5\cdot10^{-6}$ deg^{-1}; $h_s=1.2\cdot10^{-2}$ cal/(cm^2·sec·deg);

c_{ps}=0.33 cal/(g·deg); $E=5\cdot10^4$ kg/mm^2; ν=0.25; $V_0=3.3\cdot10^{-3}$ cm/sec.

It should be noted that the chosen heat-transfer coefficient takes into account the overall heat removal by radiation and convection.

2. Basic Results and Discussion. A typical distribution of the meridian σ_m and hoop σ_φ normal stresses in a longitudinal section of the tube is shown in Figs. 1 and 2. The length of the grown tube is l = 15 cm for the screen height of l^*= 8 cm. For clarity the same figures show the stresses in tubes at the same ambient temperatures near the crystallization front T_1^0 and T_3^0 and near the upper end of the tube T_5^0 and T_6^0 but in the absence of the screen. As is evident from the figures, the presence of the screen gives rise to a "burst" of stresses, which rapidly drops with distance from l^*. Although the values of the stresses near l^* can be very large, in return in this case the maximal values of the stresses become roughly half as large.

For a tube which is entirely in the screen zone we perform a subsequent analysis of the behavior of the stresses as a function of the heat transfer conditions, the tube thickness, and the value of the middle radius. An increase in the heat transfer naturally increases the temperature drop across the tube wall. Near the crystallization front at T_1^0=2000°C and T_3^0=1950°C the radial temperature gradients do not exceed 10–15 °C/cm. At T_1^0=1900 °C the radial temperature gradients attain 70°C/cm. Correspondingly, the maximal hoop stresses on the lower end of the crystal (crystallization front) in both cases for a tube 5 cm long have the values $|\sigma_\varphi|$=5.12 and 16.4kg/mm^2. Near the crystallization front and the upper end of the tube there are small regions where the normal stresses σ_φ rapidly change from negative to positive values and then decrease to values close to zero, remaining such over practically the entire length of the tube.

The largest values of the stresses $|\sigma_\varphi|$ are attained on the crystal ends, and the largest values of $|\sigma_m|$ are attained near the ends on the tube surface, and their behavior will be considered.

We denote the maximal value of $|\sigma_\varphi|$ on the crystallization front by $|\sigma_\varphi^b|_{\max}$, that on the upper end of the tube by $|\sigma_\varphi^t|_{\max}$, and the maximal values of $|\sigma_m|$ near the lower and upper ends of the tube, respectively, by $|\sigma_m^b|_{\max}$ and $|\sigma_m^t|_{\max}$.

Figure 3 shows the dependences of $|\sigma_\varphi^b|_{\max}$, $|\sigma_\varphi^t|_{\max}$, $|\sigma_m^b|_{\max}$, $|\sigma_m^t|_{\max}$ on the length of the grown crystal. From the shown plots it is evident that, beginning from some length (3.5 cm), the stresses $|\sigma_\varphi^b|_{\max}$ and $|\sigma_m^b|_{\max}$ are almost constant and the stresses $|\sigma_\varphi^t|_{\max}$ and $|\sigma_m^t|_{\max}$ rapidly decrease. On a small length (up to 3.5 cm) there are portions of drastic growth and reduction of all stresses, their values not being smaller than on lengths larger than 3.5cm. Therefore, at the initial stage of growth, when the crystal has a small length, the influence of the stresses σ_φ^t and σ_m^t near the upper end is important for the formation of the crystal structure. Since with an increase in the tube length these stresses are removed, then, beginning with some length, the influence of these stresses on the crystal structure will be insignificant. Thus, the conditions of formation of the dislocation structure with allowance for polygonization and the block structure in tubes grown from a small bar seed and those built-up on a long tubular seed crystal with the same diameter are substantially different. The obtained results permit the conclusion that when growing tubes it is preferable to take a tubular seed; its length should not be smaller than some length (in this specific case 3.5 cm).

We traced the dependences of $|\sigma_\varphi|_{\max}$ and $|\sigma_m|_{\max}$ on the middle radius of the tube R with a constant tube wall thickness h. It turned out that an increase in the radius produces a substantial increase in the stress $|\sigma_\varphi|_{\max}$, the change in the stress $|\sigma_m|_{\max}$ being insignificant.

Apart from this, the dependences of these stresses on the wall thickness h with constant R were investigated. Calculations showed that the stresses $|\sigma_\varphi|_{\max}$ and $|\sigma_m|_{\max}$ monotonically decrease as the tube wall thickness increases.

A calculation of stresses can be performed on the basis of experimentally determined values of $\Theta_1(z)$ and $\Theta_2(z)$. Besides, by varying these dependences it is possible to determine the optimal temperature distribution along the furnace for obtaining the minimal stresses in the tube with heat removal which is sufficient to realize the crystallization process.

CONCLUSIONS

1. The behavior of thermoelastic stresses is substantially different in building up a crystal on a small bar seed or on a long tubular seed, whose transverse dimension corresponds to the grown crystal.

2. To grow a tube it is preferable to take a tubular seed; its length should not be smaller than some value.

3. An increase in the heat transfer from the lateral surfaces of the tube causes an increase in the maximal hoop and meridian stresses.

4. As the length of the grown tube increases, stabilization of the hoop stress on the crystallization front and of the maximal meridian stress near the front occurs.

5. As the wall thickness increases, the level of the maximal values of the hoop and meridian stresses falls. An increase in the tube diameter at a constant tube thickness causes an increase in the hoop stress and practically does not change the value of the meridian stress.

NOTATION

T, temperature; T_m^0, melting temperature; k_s, thermal conductivity coefficient; α_t, thermal expansion coefficient; c_{ps}, heat capacity; h_s, heat-transfer coefficient; E, Young's modulus; ν, Poisson coefficient; V_0, growth rate; Θ_1, Θ_2, temperatures of the external medium; σ_m, normal meridian stress; σ_φ, normal hoop stress; u, ω, axial and radial travels of the middle surface; R_1, R_2, inner and outer radii of the tube; ρ, density.

REFERENCES

1. R. E. Novak, R. Metzl, A. Dreeben, et al., J. Cryst. Growth, **50**, 143-150 (1980).
2. K. Wada and K. Hoshikawa, J. Cryst. Growth, **50**, 151-156 (1980).
3. R. E. Novak and K. M. Kim, J. Cryst. Growth, **50**, 330-339 (1980).
4. P. I. Antonov, V. M. Krymov, and V. S. Yuferev, 7th All-Union Conference on Crystal Growth [in Russian], Moscow (1988).
5. Ya. S. Podstrigach and R. N. Shvets, Thermoelasticity of Thin Shells [in Russian], Kiev (1978).